People's Democratic Republic of Algeria
الجمهورية الجزائرية الديمقراطية الشعبية

MINISTRY OF HIGHER EDUCATION AND SCIENTIFIC RESEARCH

HIGHER SCHOOL IN APPLIED SCIENCES
--T L E M C E N--

المدرسة العليا في العلوم التطبيقية
École Supérieure en Sciences Appliquées

وزارة التعليم العالي والبحث العلمي

المدرسة العليا في العلوم التطبيقية
-تلمسان-

End of study thesis

For obtaining the Master's degree

Field: **Electrotechnics**
Speciality: **Energy and environment**

Presented by:

Mounir Amine BAKIR
Marwa DOUANE

Theme

Voltage Oriented Control of three phase PWM Converters

Publicly defended on 01/07/2024, before the jury composed of:

Mr M. Mehamedi	MAA	ESSA. Tlemcen	President
Mr A. Chemidi	MCA	ESSA. Tlemcen	Thesis Supervisor
Mr A. Tahour	Professor	ESSA. Tlemcen	Examinator 1
Mr F. Oudjama	MAB	ESSA. Tlemcen	Examinator 2

College year: 2023/2024

بِسْمِ اللَّهِ الرَّحْمَٰنِ الرَّحِيمِ

Acknowledgments

First of all, we thank ALLAH almighty for giving us the courage and patience during all these years of study.

I would like to take this chance to express my heartful gratitude and sincere appreciation to our supervisor Mr. Abdelkarim CHEMIDI. From the moment we started this work to our thesis defense, he has provided valuable feedback that pushed us to take this work further than we thought it could go, His impressive knowledge, technical skills and human qualities have been a source of inspiration and a model for me to follow.

Our most sincere thanks are addressed to Mr. M. MEHAMEDI, Assistant master class A at ESSA Tlemcen, for agreeing to chair the jury.

Our sincere thanks also go to the members of the jury Mr. Ahmed TAHOUR Professor at ESSAT, Mr. F. OUDJAMA Assistant master class B for their interest in our study and for doing us the honor of participating in this jury and enrich it with their proposals.

Dedication

To **my mother** that I wish more than anything that you were here with me now to make you proud, but continues to be the guiding light that illuminates my path forward.

To **my father** whose selfless sacrifices and tireless efforts have been the driving force behind my academic pursuits.

To **my sister Imen**, standing steadfast through the best of times and the worst. Your unwavering presence has been a true gift. Through every decision, whether joyous or difficult, you have been there to lend an ear, you are not just my sister, but my confidante, my champion, and my saving grace.

To **my only brother hamza** I am forever grateful for the countless ways you have supported me, encouraged me, and believed in me. Your strength has been my strength, the one I can always count on, no matter what.

To **my little sister hanane** I just wanted to take a moment to thank you for being such an amazing sibling. You bring so much joy and love into my life, and I'm so grateful to have you.

To **Feriel Khadidja RAHALI**, my partner in crime, I'm thrilled that our paths crossed, as we've shared countless precious moments and created unforgettable memories over the past few years, from our spontaneous road trips to our late-night conversations about life and everything in between. It was a turning point for me and I will always cherish the lessons I learned from it.

To **Habiba DERKI**, the journey would have been lacking without your unwavering enthusiasm and radiant spirit, which illuminated every step and made our shared experiences truly unforgettable, it' s transformed from ordinary to extraordinary, made our shared experiences a symphony of joy and fulfilment.

To **my constant source of motivation** and support, I am grateful for the enduring bond we share, despite the distance between us. Your continuous commitment to me has been a ray of hope and I am deeply thankful for the unshakeable faith you have on me.

To **my partner Mounir**, this thesis is the fruit of our efforts and our passions and a testimony of our collaboration.

Marwa DOUANE

Dedication

I have the pleasure of dedicating this work to

To my father, this work is dedicated to you, my father who left this world who allowed me to discover this profession of engineer and who encouraged me to follow the same path as you.

To my mother, for your support, your affection and your limitless love, your unwavering trust, your infinite patience and your immeasurable sacrifices, I humbly dedicate this work to you.

To my sister, for her encouragement and kindness that she gave me, I express my deep gratitude and my great respect. This dedication humbly offered is a testimony of the immeasurable love I have for you.

To my best friends and to all those who love me and whom I love,

To my partner Marwa who contributed to the completion of this work.

Mounir Amine BAKIR

Abstract

This thesis presents a comprehensive study on the design and implementation of a voltage-oriented control strategy for a three-phase PWM rectifier. The control strategy is designed to achieve unity power factor and maintain the DC-bus voltage at the desired level, improving the control performance of the rectifier. The proposed control scheme has been founded on the transformation between stationary and synchronously rotating coordinate system, it is based on decoupled current controller designed along with a Pulse Width Modulation consisting of a current controller and a DC-link voltage controller. The proposed scheme has been implemented and simulated in MATLAB/Simulink environment, the results obtained show the validity of the model and its control methods compared with other strategies.

Keywords: PWM rectifier, voltage oriented control VOC, decoupled control, pulse width modulation (PWM), DC-link voltage.

Résumé

Cette thèse présente une étude approfondie sur la conception et la mise en œuvre d'une stratégie de contrôle orientée tension pour un redresseur PWM triphasé. La stratégie de contrôle est conçue pour atteindre un facteur de puissance unitaire et maintenir la tension du bus CC au niveau souhaité, améliorant ainsi les performances de contrôle du redresseur. Le schéma de contrôle proposé a été fondé sur la transformation entre un système de coordonnées stationnaire et à rotation synchrone. Il est basé sur un contrôleur de courant découplé conçu avec une modulation de largeur d'impulsion composée d'un contrôleur de courant et d'un contrôleur de tension de liaison CC. Le schéma proposé a été implémenté et simulé dans l'environnement MATLAB/Simulink, les résultats obtenus montrent la validité du modèle et de ses méthodes de contrôle par rapport à d'autres stratégies.

Mots clés : redresseur PWM, contrôle orienté tension VOC, contrôle découplé, modulation de largeur d'impulsion (PWM), tension du circuit intermédiaire.

ملخص:

تقدم هذه الأطروحة دراسة شاملة حول تصميم وتنفيذ استراتيجية التحكم الموجهة بالجهد لمقوم ثلاثي الطورPWM.

تم تصميم استراتيجية التحكم لتحقيق عامل قدرة الوحدة والحفاظ على جهد ناقل التيار المستمر عند المستوى المطلوب، مما يحسن أداء التحكم في المقوم. تم تأسيس مخطط التحكم المقترح على التحول بين نظام الإحداثيات الثابت والمتحرك بشكل متزامن، وهو يعتمد على وحدة تحكم التيار المنفصلة المصممة جنبًا إلى جنب مع تعديل عرض النبض الذي يتكون من وحدة تحكم التيار ووحدة تحكم الجهد ذات الارتباط المستمر. تم تنفيذ ومحاكاة المخطط المقترح في بيئة MATLAB/SIMULINK

وأظهرت النتائج التي تم الحصول عليها صلاحية النموذج وطرق التحكم به مقارنة مع الاستراتيجيات الأخرى.

الكلمات المفتاحية:

مقوم PWM ،التحكم الموجه بالجهد VOC ،التحكم المنفصل ، تعديل عرض النبضة PWM، جهد وصلة DC

Abbreviations

AC: Alternating Current

DC: Direct Current

AFE: Active front-end

IGBT: Insulted gate bipolar transistors

THD: total harmonic distortion

LCL: line commutated low-pass

PWM: pulse width modulation

PFC: power factor correction

UBC: universal bridge converter

UPF: unity power factor

SPWM: modulation by sinusoidal pulse width

PLL: phase locked loop

HB: hysteresis band

VOC: voltage oriented control

DPC: direct power control

VFOC: virtual flux oriented control

VF-DPC: virtual flux direct power control

IM: induction motor

VSC: voltage source converters

SVM: space vector modulation

PI: proportional integral

IMC: internal model control

List of Figures

List of Tables

Table of Contents

General introduction

For recent decades, an increasing amount of the electric energy produced is converted through rectifiers before the consumption at its final load. Three-phase AC-DC converters are widely used in many different areas such as adjustable-speeds drive, battery charging for electric vehicles and wind energy conversion systems, etc.

Diodes and thyristors bridge rectifiers are conventionally used in power electronics field as a first stage of conversion, but they nonlinear in nature, consequently they become a major source of high voltage and current total harmonic distortion resulting low power factor of the load. A number of problems in the power distribution system appears such as an increasing of reactive power and power losses in transmission lines, voltage distortion, electromagnetic and increasing voltampere ratings of the power system equipment (generators, transformers etc).

Thus, a new generation of controlled rectifiers have been developed which is three-phase PWM rectifiers. They basically offer three fascinating features such as high power factor, low harmonic pollution and bi-directional power flow, the line-side converter operates as rectifier in forward energy flow, and as inverter in reverse energy flow. These PWM converters have become recently an interesting research subject in renewable power generation systems.

Various control strategies of the PWM rectifiers have been presented in recent researches Among of them the voltage oriented vector control is considered as the most common method due to its high dynamic operation. This thesis aims to study, model and simulate a three phase PWM rectifier based on voltage oriented control strategy, to improve its performance converting AC to DC voltage and the system's robustness and dynamic response of the dc- bus voltage

The first chapter is an overview of three phase PWM controlled rectifiers, it present a several topologies with their features, a modelling of chosen universal bridge topology in both three phase and two-phase references and pulse width modulation control technique.

The second chapter contains various control strategies of the PWM rectifiers which can be classified in two categories, voltage based and virtual flux based control. A mathematical model of three–phase voltage oriented control PWM rectifier is presented in the three-phase coordinates and the two-phase stationary coordinates, then a study on the mentioned control strategy is carried on.

The last chapter present a simulation results of the PWM rectifier with different control strategies to achieve the appropriate technique for AC to DC conversion system.

Chapter I

THREE PHASE CONTROLLED RECTIFIER

I.1. Introduction

The entire Wind energy conversion system under study is a complicated system made up of several essential components.

In wind turbine systems, an increasing percentage of the generated electric energy is converted through rectifiers (three phase rectifier), before it is used at the final load. They enable effective conversion of the three-phase alternating current (AC) voltage produced by the wind turbine into direct current (DC) voltage. This conversion is accomplished by means of controlled switching of high-power semiconductor devices.

In the section that follows, we will examine various three-phase rectifier topologies, focus on Universal bridge topology.

I.2. Topologies

I.2.1. Three-phase full-wave bridge rectifier

This is the simplest topology, consisting of a bridge arrangement of diodes, it offers full-wave rectification. Although it offers full-wave rectification, there is no control over the output voltage or power factor, its major harmonic distortion and low power factor might lead to grid instability.

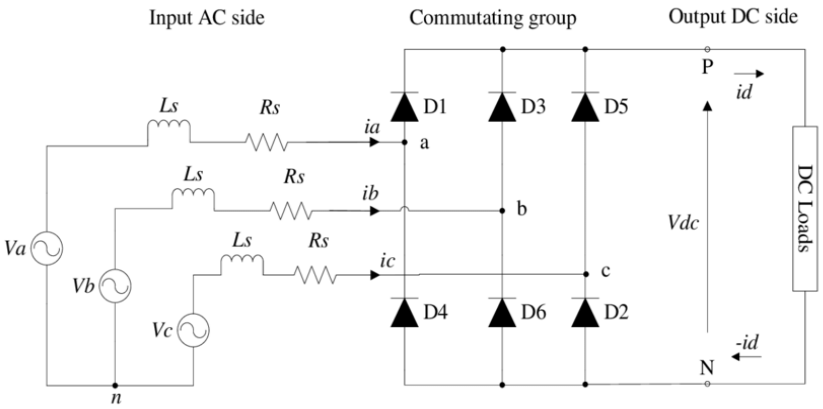

Figure I.1: Three-phase full-wave bridge rectifier [1].

I.2.2. Active Front-End (AFE) Rectifier

AFE is referred to "Active Front-End" rectifier, because it is an active power electronic device which used at the front end of an AC/ DC power converter system, it allows for bidirectional power flow and actively regulate the input current waveform and shape it to be sinusoidal by

employing Insulated Gate Bipolar Transistors (IGBTs) in place of diodes in the rectifier component, to achieve low total harmonic distortion (THD) and high-power factor [2]. Compared to conventional diode-based rectifiers, this significantly lowers the total harmonic distortion (THD) to 5% or less. The main drawback is that AFE rectifiers require an LCL filter to reduce higher-order harmonics caused by the switching frequency of the IGBTs, which adds to the cost and complexity of the system [3].

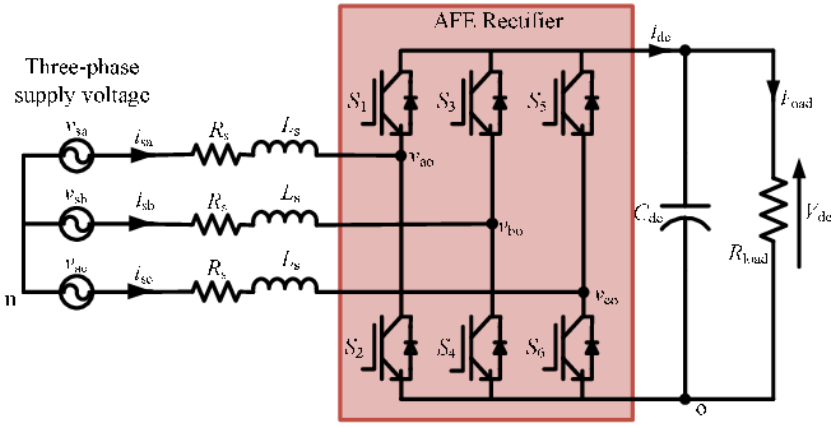

Figure I.2: Active Front-End Rectifier [4].

I.2.3. Vienna Rectifier

The Vienna Rectifier is a unidirectional three-phase three-switch three-level Pulse-width modulation (PWM) rectifier. It is equal to a three-phase diode bridge with a built-in boost converter [5], it's able to function with a three-wire input without a connection to neutral, produce a controlled output voltage. But the Vienna Rectifier can generate harmonic distortion in the input current, which can lead to resonance problems in the system. This can affect the stability and performance [6].

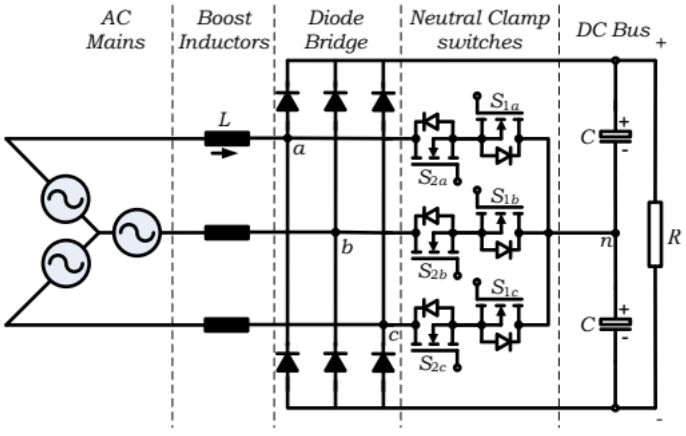

Figure I.3: Vienna Rectifier topology [6]

I.2.4. PWM rectifier

The PWM rectifier incorporates the power factor correction (PFC) technique to ensure that the system operates with a high-power factor.

This technique is employed to control the switching of semiconductor devices (such as IGBTs or MOSFETs) in the rectifier circuit [7]. The rectifier regulates the width of the pulses to control voltage and current to match the requirements of the connected load. Because of this, they have a low potential cost and merely offer the option of active filtering or regenerative braking mode.

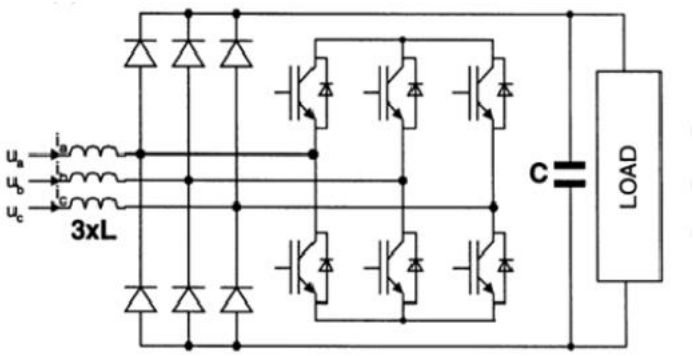

Figure I.4: PWM rectifier [8].

I.2.5. Universal Bridge Topology

Usually referred to as the Universal Bridge Converter (UBC), this adaptable power conversion topology contains elements of both rectifiers and inverters. It offers bidirectional power flow capability, allowing it to operate in both rectification and inversion modes. can be implemented with up to six power switches connected in a bridge configuration like IGBTs, MOSFETs, diodes, and thyristors, and it can also provide a unity power factor (UPF). However, its disadvantages are a high per-unit current rating, poor immunity to shoot-through faults, and high switching losses [9].

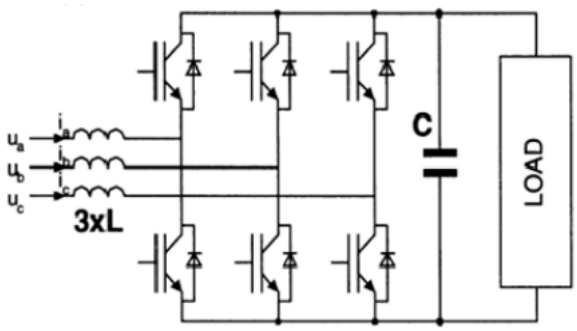

Figure I.5: The Universal Bridge Topology [8].

I.3. Three-phase rectifier topologies, performance comparison

The following table compares between the performance of previous topologies according to their features.

Table I.1: Features of three-phase rectifiers

FEATURE TOPOLOGY	REGULATION OF DC OUTPUT VOLTAGE	LOW HARMONIC DISTORSION OF LINE CURRENT	NEAR SINUSOIDAL CURRENT WAVEFORMS	POWER FACTOR CORRECTION	BIDIREC-TIONAL POWER FLOW	UNITED FACTOR POWER
Topology 01	-	-	-	-	-	-
Topology 02	-	+	-	+	+	-
Topology 03	+	+	+	+	+	-
Topology 04	+	+	-	+	+	-
Topology 05	+	+	+	+	+	+

I.4. Universal bridge topology

I.4.1. Mathematical model

The voltage and current of the three-phase line are [9]:

$$\begin{aligned} u_a &= E_m cos(\omega t) \\ u_b &= E_m cos(\omega t - \tfrac{2\pi}{3}) \\ u_c &= E_m cos(\omega t - \frac{4\pi}{3}) \end{aligned} \tag{I.6}$$

$$\begin{aligned} i_a &= I_m cos(\omega t + \varphi) \\ i_b &= I_m cos(\omega t + \varphi - \tfrac{2\pi}{3}) \\ i_c &= I_m cos(\omega t + \varphi - \frac{4\pi}{3}) \end{aligned} \tag{I.7}$$

We have also:

$$i_a + i_b + i_c = 0 \tag{I.8}$$

We call a space vector the quantity

$$v^s(t) = v_\alpha(t) + jv_\beta(t) = \frac{2}{3}K\left(v_a(t) + v_b(t)e^{j\frac{2\pi}{3}} + v_c(t)e^{j\frac{4\pi}{3}}\right) \quad \text{(I.9)}$$

where K is a scaling constant (amplitude invariant k=1, RMS-invariant k= $1/\sqrt{2}$, power invariant $k = \sqrt{\frac{3}{2}}$

I.4.2. RECTIFIER ABC-MODEL

$$\boldsymbol{u_{Sab} = (S_a - S_b)u_{dc}}$$

$$\boldsymbol{u_{Sbc} = (S_b - S_c)u_{dc}} \quad \text{(I.10)}$$

$$\boldsymbol{u_{Sca} = (S_c - S_a)u_{dc}}$$

with S_i are the switching functions defined by $S_i = \begin{cases} 1 & upper\ switch\ ON \\ 0 & bottom\ switch\ ON \end{cases}$ with i=a, b, c

We obtain:

$$\begin{aligned} u_{Sa} &= f_a.u_{dc} \\ u_{Sb} &= f_b.u_{dc} \\ u_{Sc} &= f_c.u_{dc} \end{aligned} \quad \text{(I.11)}$$

$$f_a = S_a - S^* = S_a - \frac{1}{3}(S_a + S_b + S_c) = \frac{2S_a - (S_b + S_c)}{3}$$

$$f_b = S_b - S^* = S_b - \frac{1}{3}(S_a + S_b + S_c) = \frac{2S_b - (S_a + S_c)}{3} \quad \text{(I.12)}$$

$$f_c = S_c - S^* = S_c - \frac{1}{3}(S_a + S_b + S_c) = \frac{2S_c - (S_a + S_b)}{3}$$

$$(f_{abc}\ are\ 0, \pm 1/3\ or\ \pm 2/3)$$

The rectifier in defined by four equations

Three for each voltage phase:

$$\begin{bmatrix} u_a \\ u_b \\ u_c \end{bmatrix} = R\begin{bmatrix} i_a \\ i_b \\ i_c \end{bmatrix} + L\frac{d}{dt}\begin{bmatrix} i_a \\ i_b \\ i_c \end{bmatrix} + \begin{bmatrix} u_{Sa} \\ u_{Sb} \\ u_{Sc} \end{bmatrix} \quad \text{(I.13)}$$

And one for the dc-link currents:

$$C\frac{du_{dc}}{dt} = S_a i_a + S_b i_b + S_c i_c - i_{load} \quad \text{(I.14)}$$

A representation of a block diagram can be created by combining the previous formulas in figure I.10 [9].

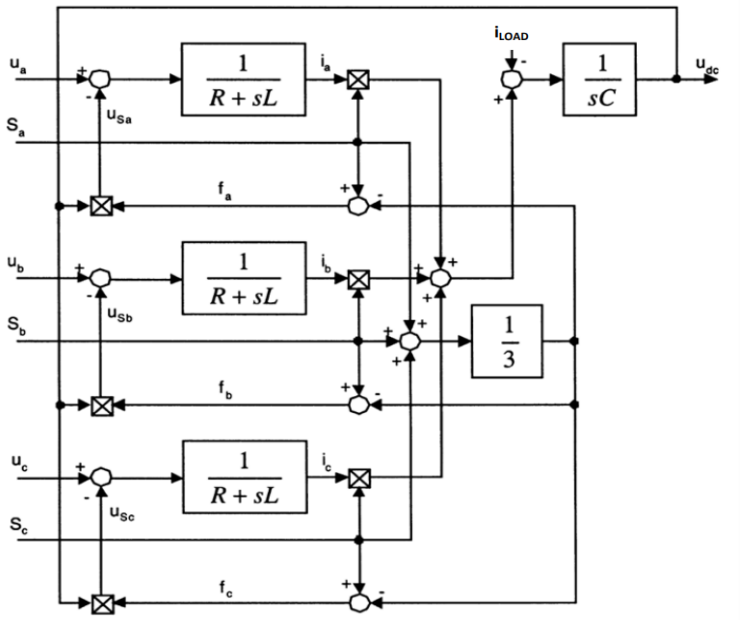

Figure I.6: Block diagram of voltage source PWM rectifier in natural three-phase coordinates

I.4.3. RECTIFIER αβ-EQUATIONS

Applying Clarke transformation, we find the voltage equations in αβ-coordinates, the amplitude invariant Clarke transformation is mentioned in (I.4.1):

$$\begin{bmatrix} \boldsymbol{u_\alpha} \\ \boldsymbol{u_\beta} \end{bmatrix} = \boldsymbol{R}\begin{bmatrix} \boldsymbol{i_\alpha} \\ \boldsymbol{i_\beta} \end{bmatrix} + \boldsymbol{L}\frac{\boldsymbol{d}}{\boldsymbol{dt}}\begin{bmatrix} \boldsymbol{i_\alpha} \\ \boldsymbol{i_\beta} \end{bmatrix} + \begin{bmatrix} \boldsymbol{u_{S\alpha}} \\ \boldsymbol{u_{S\beta}} \end{bmatrix} \quad \text{(I.15)}$$

$$C\frac{\boldsymbol{du_{dc}}}{\boldsymbol{dt}} = \frac{\boldsymbol{3}}{\boldsymbol{2}}(\boldsymbol{S_\alpha i_\alpha} + \boldsymbol{S_\beta i_\beta}) - \boldsymbol{i_{load}} \quad \text{(I.16)}$$

I.4.4. RECTIFIER dq-EQUATIONS

Now, we move to the Park transformation which is:

$$v_{dq} = v^s e^{-j\theta} \quad \text{(I.17)}$$

where v^s is a space vector ($v^s = v_\alpha + jv_\beta$). Hence

$$u^s = Ri^s + L\frac{di^s}{dt} + u_S^s \tag{I.18}$$

$$u_{dq}e^{j\theta} = Ri_{dq}e^{j\theta} + L(e^{j\theta}(j\omega i_{dq} + \frac{di_{dq}}{dt})) + e^{j\theta}u_{Sdq}$$

$$u_{dq} = Ri_{dq} + L\frac{di_{dq}}{dt} + jL\omega i_{dq} + u_{Sdq} \tag{I.19}$$

For last, by separating the Real and Imaginary parts, we get

$$u_d = Ri_d + L\frac{di_d}{dt} - \omega Li_q + u_{Sd} \tag{I.20}$$

$$u_q = Ri_q + L\frac{di_q}{dt} + \omega Li_d + u_{Sq} \tag{I.21}$$

$$\mathrm{C}\frac{du_{dc}}{dt} = \frac{3}{2}(S_d i_d + S_q i_q) - i_{load} \tag{I.22}$$

I.4.5. INSTANTANEOUS POWER

As we know the instantaneous power defined by $P = Re\{V * I^*\}$ with « * » indicates complex conjugate, So the instantaneous power for three-phase system will

be proportional to

$$Re\{v^s(i^s)^*\} = Re\{v^{dq}(i^{dq})^*\} \tag{I.23}$$

It is noted that the formula is independent of the coordinate system.

From the space vector relation, we obtain:

$$v^s(i^s)^* = \left(\frac{2}{3}K\right)^2 \left(v_a + v_b e^{j\frac{2\pi}{3}} + v_c e^{j\frac{4\pi}{3}}\right)\left(i_a + i_b e^{j\frac{2\pi}{3}} + i_c e^{j\frac{4\pi}{3}}\right)^*$$

$$= \left(\frac{2}{3}K\right)^2 \left[v_a i_a + v_b i_b + v_c i_c + j\frac{1}{\sqrt{3}}(v_a(i_c - i_b) + v_b(i_a - i_c) + v_c(i_b - i_a)\right]$$

The Real part gives us the active power

$$P = \frac{3}{2K^2}Re\{v^s(i^s)^*\} = \frac{3}{2K^2}Re\{v^{dq}(i^{dq})^*\} = v_a i_a + v_b i_b + v_c i_c \tag{I.24}$$

When we obtain the reactive power with imaginary part

$$Q = \frac{3}{2K^2} Im(v^s (i^s)^*) = \frac{3}{2K^2} Im\{v^{dq} (i^{dq})^*\}$$

$$= \frac{1}{\sqrt{3}} [v_a (i_c - i_b) + v_b (i_a - i_c) + v_c (i_b - i_a)] \quad \text{(I.25)}$$

For ideal, positive sequence space vectors, we take

$$v^s = KE_m e^{j\omega t} \; and \; i^s = KI_m e^{j\omega t + \varphi}$$

Where E_m and I_m are amplitudes

The active power relation is

$$P = \frac{3}{2K^2} Re\{v^s (i^s)^*\} = \frac{3}{2K^2} Re\{v^{dq} (i^{dq})^*\} = \frac{3}{2} E_m I_m cos\varphi = 3VIcos\varphi \quad \text{(I.26)}$$

Where V and I are rms-values. This previous relation will be use in the DC-link voltage controller design.

I.5. Pulse Width Modulation

Pulse Width Modulation (PWM) is a widely used technique for controlling the amount of power delivered to a load by varying the width of the pulse in a periodic waveform, it's used to synthesize pseudo-analogy signals using digital circuits (all or nothing, 1 or 0). The principle is to create a logical signal (value 0 or 1), with a fixed frequency but whose cyclic ratio (duty cycle) is numerically controlled. The output signal of the pulse width modulator is a square-wave pulse, of constant frequency and variable pulse duty ratio. If the amplitude of the output signal of the amplifier is greater than that of the reference signal, then there will be a high signal at the output of the pulse width modulator; if it is less, there will be a Low signal [10].

I.5.1. Modulation by Sinusoidal Pulse Width SPWM

Sinusoidal pulse width modulation is a specific PWM technique in which the reference wave shape is a sinusoid. In the SPWM, voltage impulses are modulated to reproduce the sinusoidal wave shape of the output voltage as precisely as possible. This method aims to reduce the harmonics and improve the quality of the output voltage compared to other forms of PWM.

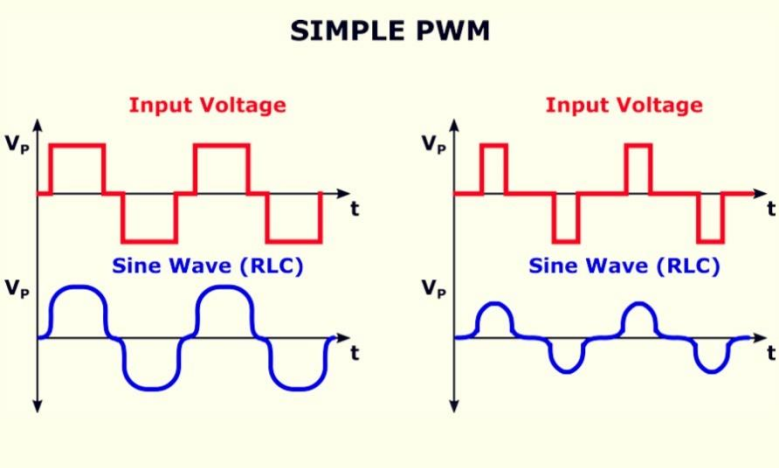

Figure I.7: Sinusoidal PWM [11]

I.5.2. The sinusoidal triangular PWM

involves comparing a triangular carrier signal with a reference signal, such as a sine wave, to generate a Pulse Width Modulated (PWM) signal. This method allows for the modulation of the duty cycle of the PWM signal based on the comparison between the carrier signal and the reference signal. By using this approach, it becomes possible to control the average power or amplitude delivered to a load, making it a valuable method for applications like controlling power to motors or other analogy devices.

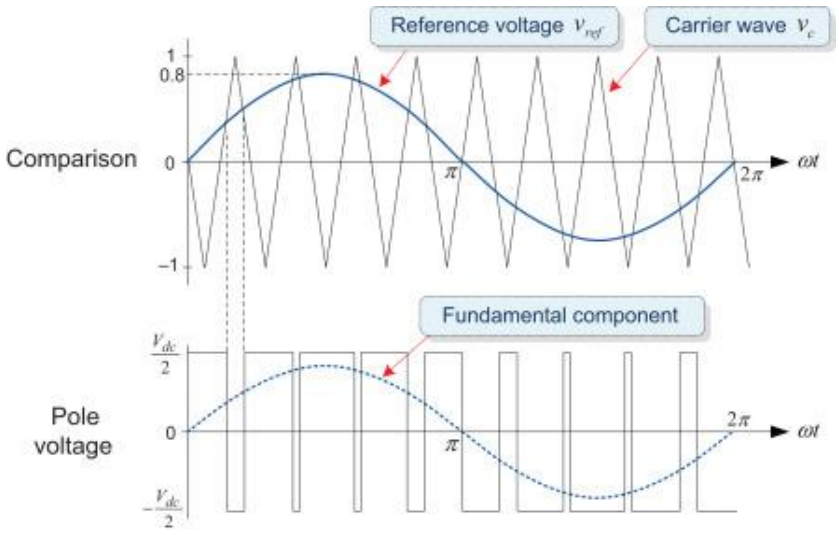

Figure I.8: sinusoidal triangular PWM [12]

The carrier uses a triangular wave because it gives less current ripple compared to other carrier waves, if the reference value is higher than the carrier waves the switch is s=1 and if it is below

the switch s=0, therefore the phase potential for each line is modulated between $\pm u_{dc}/2$ as show in Figure (I.13) [10].

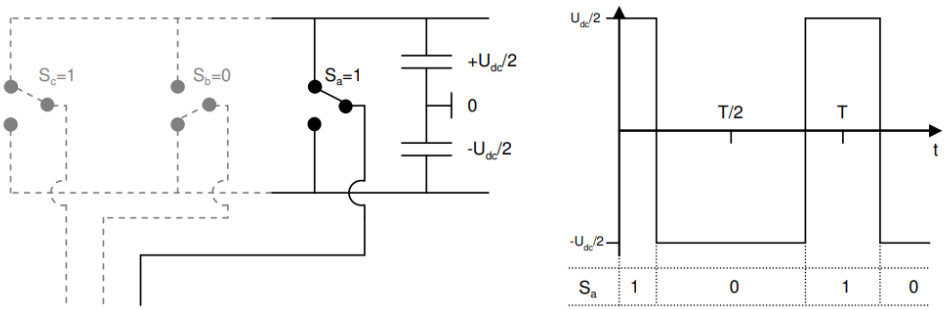

Figure I.9: Converter switch and output line voltage for one phase [10]

I.6. Three-phase pulse width-modulated rectifiers

PWM (Pulse Width Modulation) rectifier is an AC to DC power converter that uses forced commutated power electronic semiconductor switches, such as insulated gate bipolar transistors (IGBTs), to control the output voltage and power factor. allows for bidirectional power flow, enabling features like regenerative braking in frequency converters. The main advantage of using PWM is the reduction of higher-order harmonics, allowing for better control of the output voltage magnitude and improved power factor [13].

This is achieved by forcing the switches to follow the input voltage waveform using a phase-locked loop (PLL) control system. PWM rectifiers can achieve very low total harmonic distortion (THD) of the input current, typically around 1-2%.

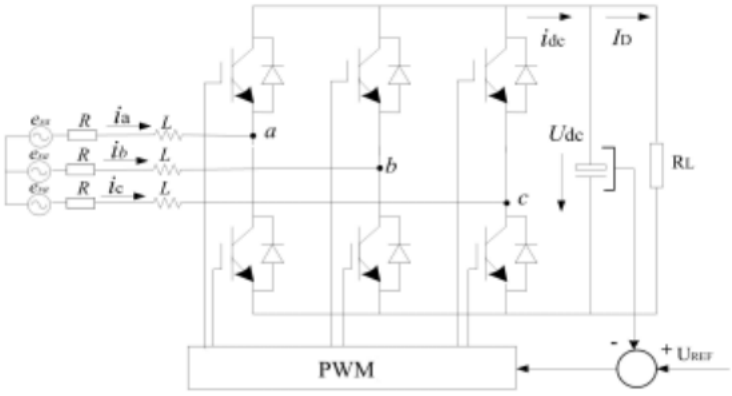

Figure I.10: main circuit of three phase PWM rectifier [13]

I.7. PWM hysteresis control

It is an effective technique for three-phase PWM rectifiers to achieve near-unity power factor and regulated DC output voltage. The hysteresis current control method produces a variable switching frequency, with the switching frequency range typically between 18-48 kHz.

This helps reduce harmonics and improve the quality of the input current waveform. The hysteresis control adjusts the PWM switching signals based on the difference between the actual and reference current, maintaining the current within a hysteresis band. This provides good dynamic performance and stability.

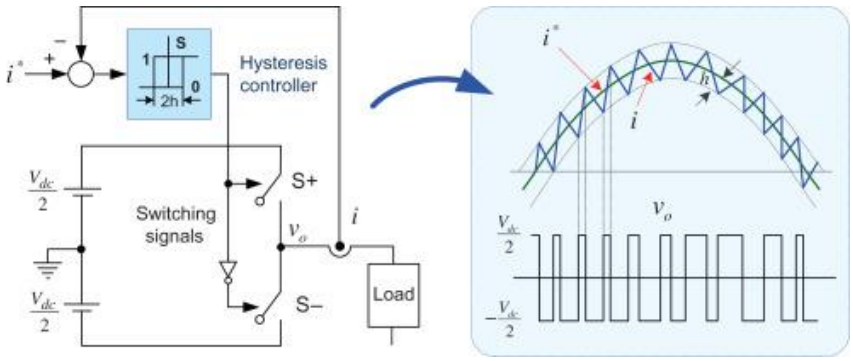

Figure I.11: Hysteresis controller [12]

This technique adjusts the PWM switching signals based on the difference between the actual and reference current, maintaining the current within a hysteresis band (HB).

I.8. Conclusion

In this chapter, we have shed light on the three phase controlled rectifiers. The chapter is divided into several sections, each focusing on a specific aspect. The first section discusses the different three-phase rectifier topologies and compares them based on features. We then we select the most suitable configuration: the universal bridge topology, which is an interesting configuration for three-phase power conversion. This topology is further detailed through the presentation of its mathematical model and its transformations to control behaviour of the rectifier. The second section explores the principles of PWM, and the concept of PWM hysteresis control, which is a popular method for implementing PWM in three-phase rectifiers.

In the next chapter we will, introduce some techniques of controlling a PWM converters, select the voltage oriented control by figuring out its features and modelling it to control and increase the performance of the system.

Chapter II

Voltage oriented control

II.1. Introduction

The advancements in power electronics, increasing energy consumption and the flexibility of semiconductor utilization have been recently receive significant attention of researchers. Generally, basic diode inverters absorb a no sinusoidal current and cause harmonics pollution and sometimes consume reactive energy. As a result, the shape of the source current wave loses its sinusoidal form and causes a low power-factor.

The control of PWM rectifier is a common problem as controlling a PWM inverter. Several techniques for controlling a PWM converters are appears, seeks for a reduced harmonic distortion and a precise power control [14]. These techniques are classified based on their principles in two classes, techniques based on the voltage and others based on the virtual-flux. For the techniques which are based on the voltage, in this chapter we will be interested in Voltage-oriented control strategy (VOC), it is a control strategy used in power electronics, particularly for controlling voltage source converters. In a variety of applications, including motor drives, renewable energy systems, and grid-connected systems. VOC's primary objective is to control the output voltage or current waveforms in accordance with the desired reference values by regulating the DC-link voltage.

The main goal of controlling the system is to maintain the dc-link voltage (V_{dc}) at the required level, while currents drawn from the power system should be ideally sinusoidal to satisfy the unity power factor condition.

II.2. Control strategies

Different control strategies for this type of PWM converter have been presented in recent research. These control techniques can lead to the same major goals, such as the high-power factor and near-sinusoidal current waveforms, but their principles are varied.

Generally, PWM rectifier control strategies can be classified using two types of estimations, voltage based and virtual flux-based control as shown in Figure (II.1)

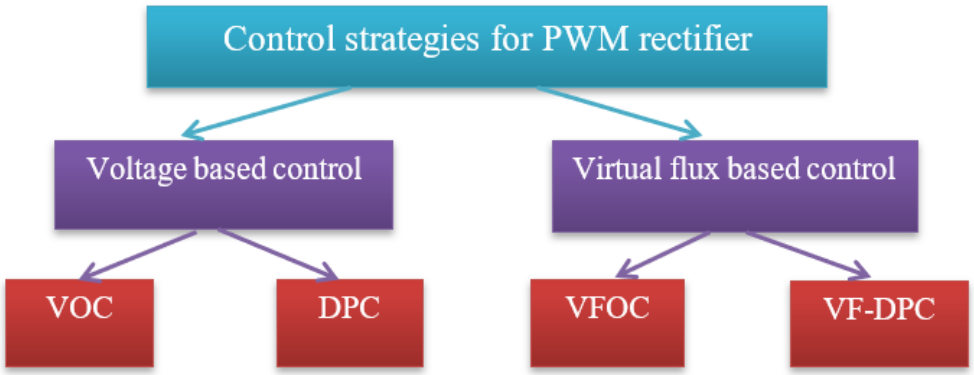

Figure II.1: PWM rectifier control strategies

Similarly, as in FOC of an induction motor, voltage-based control for PWM rectifier estimate the voltage and correct it under unbalanced conditions and pre-existing harmonic distortion [15]. For the virtual flux-based method, it corresponds to direct analogy of IM control, used to directly control the active and reactive power. In this thesis we'll choose the voltage-based control based on factors that will be explained by the following.

II.2.1. Voltage-based control methods

II.2.1.1 Voltage oriented control

This strategy is based on the idea of controlling the space vector of input AC voltage according to the position of space vector of the network voltage, which states that in order to regulate the voltage and current waveforms, the AC voltage and current vectors are oriented in the same direction by controlling the current vector in the two synchronous rotating d-q reference, it guarantees fast transient response and high static performance via an internal current control loop, has become very popular and has constantly been developed and improved ([8], [9]).

Through the use of a decoupled control of the two components of the current vector, it ensures the PWM rectifier to draw the sinusoidal line current [14].

The modelling and block diagram are in the upcoming sections of this work.

II.2.1.2 Direct Power Control (DPC)

This strategy is used to control the active and reactive power flow directly between the VSC (Voltage source converters) and the load by choosing the optimal switch state. DPC strategy chooses the proper switching state for the converter based on the power error. In order to

achieve the appropriate power exchange between the AC and DC sides, the switching state dictates how the power switches are configured in the converter circuit.

Compared with the other conventional current control strategy, it has the advantages of high-power factor, low total harmonic distortion (THD), high efficiency, and simple algorithm and program [16].

The circuit construction of the DPC strategy is illustrated in the accompanying figure:

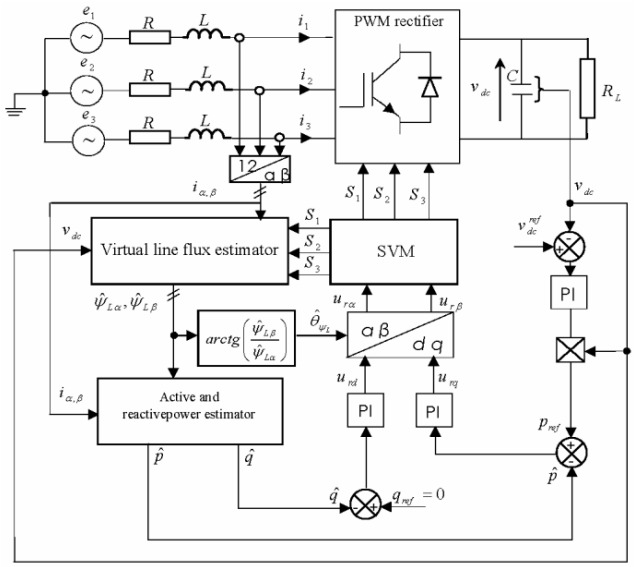

Figure II.2: Block scheme Direct Power Control [17]

In the control scheme depicted in Figure above, the reactive power reference is set to zero for unity power factor UPF consideration and the active power reference is delivered from the PI-DC voltage controller. The errors between the references and their estimated values are delivered to PI controllers. The output signals from PI controllers after transformation are used as switching signals for a space-vector modulation (SVM).

II.2.2. Virtual Flux Based Control (VFBC)

The concept is based on a duality with the induction motor. The AC-side of the PWM rectifier is assumed as a virtual motor. Then, the estimated virtual flux can be used in the control system. Therefore, the rectifier is controlled to generate the virtual flux needed to drive the desired current flowing between the converter and the grid.

In a stationary reference frame, the components of virtual line flux are estimated by the integration of line voltage U_L as follows [17]:

$$\begin{cases} \psi_{L\alpha} = \int U_\alpha dt \\ \psi_{L\beta} = \int U_\beta dt \end{cases} \quad \text{(II.1)}$$

For virtual flux voltage-oriented control, the quality of the controlled system depends on how effectively the phase-locked loop (PLL) has been designed; it uses the angle of VF vector $\gamma_{\psi L}$ because it's less sensitive to disturbances sector detection, even under operation with distorted and unbalanced line voltages, the block diagram of VF-VOC is given in the following figure [8].

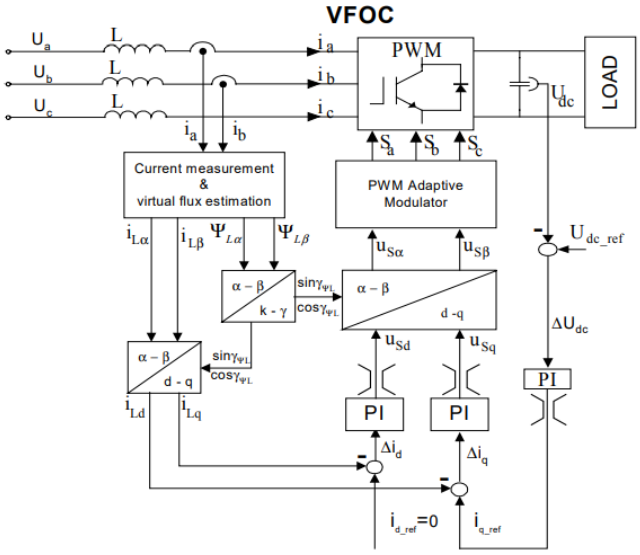

Figure II.3: Block scheme of VFOC [8]

The VF-DPC uses the estimated virtual flux to estimate instantaneous power flow in the system as can be described by the following formulas, the detailed calculation of active and reactive power is in [18]:

$$\begin{cases} P = \omega(\psi_{L\alpha} i_\beta - \psi_{L\beta} i_\alpha) \\ q = \omega(\psi_{L\alpha} i_\alpha - \psi_{L\beta} i_\beta) \end{cases} \quad \text{(II.2)}$$

i_α and i_β are line currents in stationary reference frame. Both power estimation equations are simple to calculate and do not require the computation of the current derivatives.

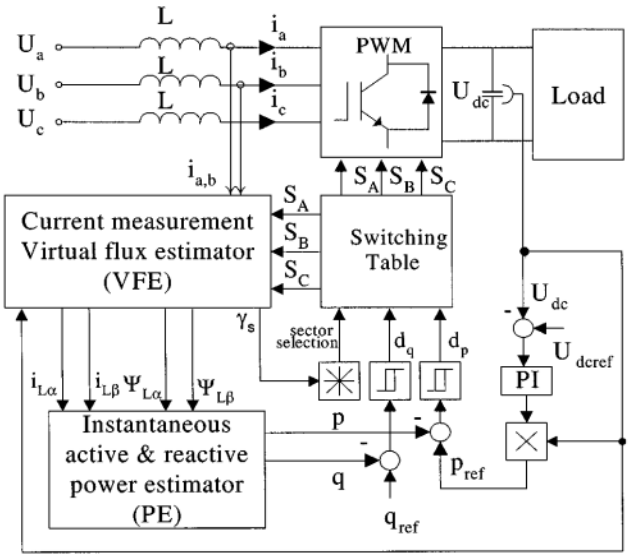

Figure II.4: Block scheme of VF-DPC. [18]

These control strategies can achieve the same main goals, such as an accurate control, high power factor and near sinusoidal input current waveforms, but it has not a good performance under harmonic conditions of the supply voltage which is the main drawback of the strategy.

II.3. Choice of strategy

Comparing the strategies of control above, we choose voltage-oriented control VOC (or Virtual field-oriented control because both methods have same advantages).

It provides a fixed switching frequency, which makes it easier to design input filters. Only VOC or VFOC can provide this feature. Additionally, VOC allows for the use of advanced PWM strategies, which can improve the efficiency and performance of the control system.
Also, as a result of a series of transformations from three phase stationary reference to a synchronous rotating reference system, the voltages remain controlled [19].

Before proceeding with the controller's design and simulation, it is necessary to clarify a few important references that were included in this study.

II.4. Comparison and discussion

The following table summarizes the main characteristics of the different control strategies ([9], [19]).

Table II.1: Control strategies comparison

Technique	Advantages	Drawbacks
VOC and VFOC	-Cheap AC/DC converters. -This control allows to use advanced PWM. -They offer a fixed switching frequency, making it easier to design input. -Low sampling frequency for good performance.	-Decoupling between active and reactive power is necessary. -VOC and VFOC use lower input factor, unlike DCP or VF-DCP controls. -Complex algorithms.
DPC	-Non-linear hysteresis controllers. -DPC is a Simple algorithm that does not require complex calculations or transformations. -Can handle disturbances and uncertainties in the system.	-Variable switching frequency -Mainly used in low-power applications due to its limited scalability -Limited to specific switching patterns such as sinusoidal pulse width modulation (SPWM)
VF-DPC	-Fixed switching Frequency (easier design input filter) - provides sinusoidal line current even when the supply voltage is not ideal, ensuring better quality of power output -VF-DPC offers low total harmonic distortion.	-Variable switching frequency -Fast microprocessor and A/D converters required -The complexity of VFDPC implementation may result in higher implementation costs compared to simpler control strategies

II.5. Voltage oriented control modelling

II.5.1 Mathematical model

Figure II.5 shows the three-phase PWM rectifier block diagram, in which e_a, e_b and e_c are the power source phase voltages, *R* and *L* are line resistance and line inductance respectively, i_a, i_b and i_c are the line currents, v_a, v_b and v_c are the AC side voltages of the rectifier, *C* is dc-link capacitor, i_{dc} is dc-link current, i_L is load current, *RL* is load resistance [20].

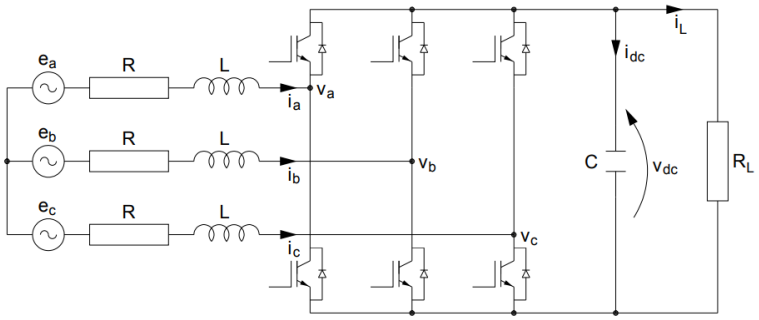

Figure II.5: Schematic diagram of a PWM rectifier [20]

3-Phase system definition

$$\boldsymbol{u_a = E_m cos(\omega t)}$$

$$\boldsymbol{u_b = E_m cos\left(\omega t - \frac{2\pi}{3}\right)} \quad \text{(II.3)}$$

$$\boldsymbol{u_c = E_m cos\left(\omega t + \frac{2\pi}{3}\right)}$$

$$\boldsymbol{I_a = I_m . cos(\omega t + \varphi)}$$

$$\boldsymbol{I_b = I_m . cos\left(\omega t + \varphi - \frac{2\pi}{3}\right)} \quad \text{(II.4)}$$

$$\boldsymbol{I_c = I_m . cos\left(\omega t + \varphi + \frac{2\pi}{3}\right)}$$

These three voltages and currents are split in two components α and β (real and imaginary respectively) [19].

$$v^s = v_\alpha + jv_\beta = \frac{2}{3}k\left(v_a + v_b e^{j\frac{2\pi}{3}} + v_c e^{-j\frac{2\pi}{3}}\right) \quad \text{(II.5)}$$

To facilitate the control, we took the amplitude invariant k=1

The α-β transformation is expressed by applying the matrix from the space vector modulation.

$$\begin{bmatrix}\alpha\\ \beta\end{bmatrix}=\begin{bmatrix}\frac{2}{3} & -\frac{1}{3} & -\frac{1}{3}\\ 0 & \frac{1}{\sqrt{3}} & -\frac{1}{\sqrt{3}}\end{bmatrix}\begin{bmatrix}a\\ b\\ c\end{bmatrix} \quad and \quad \begin{bmatrix}a\\ b\\ c\end{bmatrix}=\begin{bmatrix}1 & 0\\ -\frac{1}{2} & \frac{\sqrt{3}}{2}\\ -\frac{1}{2} & -\frac{\sqrt{3}}{2}\end{bmatrix}\begin{bmatrix}\alpha\\ \beta\end{bmatrix} \qquad \text{(II.6) (II.7)}$$

$$\begin{bmatrix}d\\ q\end{bmatrix}=\begin{bmatrix}cos\theta & sin\theta\\ -sin\theta & cos\theta\end{bmatrix}\begin{bmatrix}\alpha\\ \beta\end{bmatrix} \ and \ \begin{bmatrix}\alpha\\ \beta\end{bmatrix}=\begin{bmatrix}cos\theta & -sin\theta\\ sin\theta & cos\theta\end{bmatrix}\begin{bmatrix}d\\ q\end{bmatrix} \qquad \text{(II.8) (II.9)}$$

After transformation from ABC to αβ coordinates, the voltage equation can be expressed as follows.

$$\begin{bmatrix}u_\alpha\\ u_\beta\end{bmatrix}=R\begin{bmatrix}i_\alpha\\ i_\beta\end{bmatrix}+L\frac{d}{dt}\begin{bmatrix}i_\alpha\\ i_\beta\end{bmatrix}+\begin{bmatrix}u_{S\alpha}\\ u_{S\beta}\end{bmatrix} \qquad \text{(II.10)}$$

Physically, after the Clarke transformation, $u_\alpha \ and \ u_\beta$ are still sinusoidal signals. Changing again the reference axis onto d-q axis, by applying Park transformation, the αβ axis are displaced by the angle θ as shown in

$$v_{dq}=v^s e^{-j\theta} \qquad \text{(II.11)}$$

By applying the transformation

$$u_{dq}=Ri_{dq}+L\frac{di_{dq}}{dt}+jL\omega i_{dq}+u_{Sdq} \qquad \text{(II.12)}$$

We can obtain the equations of the system in the two-phase synchronous rotation d-q coordinate (real and imaginary part)

$$\begin{cases}\frac{di_d}{dt}=-\frac{R}{L}i_d+\omega i_q+\frac{1}{L}(e_d-v_d)\\ \frac{di_q}{dt}=-\frac{R}{L}i_q+\omega i_d+\frac{1}{L}(e_q-v_q)\\ \frac{dv_{dc}}{dt}=\frac{-v_{dc}}{CR_L}+\frac{(e_d i_d+e_q i_q)}{Cv_{dc}}\end{cases} \qquad \text{(II.13)}$$

The Figure II.6 below represents the system block diagram

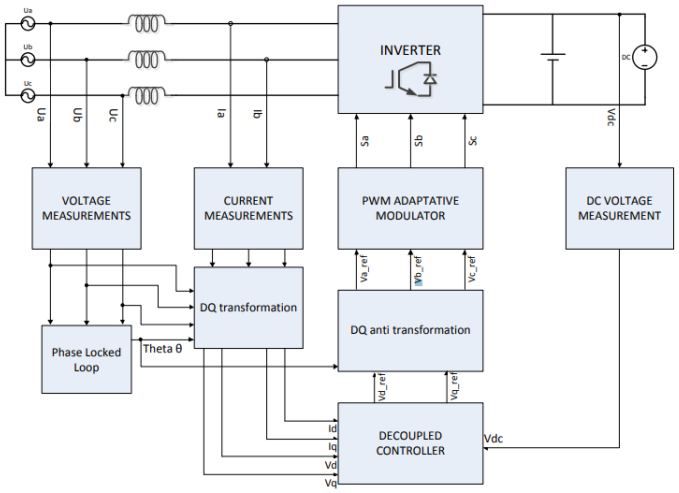

Figure II.6: configuration of VOC for PWM rectifier [19]

According to the transformations shown before, we can obtain the active and reactive power.

$$Re\{v^s(i^s)^*\} = Re\{v^{dq}(i^{dq})^*\} \tag{II.14}$$

$$v^s(i^s)^* = \left(\frac{2}{3}K\right)^2 \left(v_a + v_b e^{j\frac{2\pi}{3}} + v_c e^{j\frac{4\pi}{3}}\right)\left(i_a + i_b e^{j\frac{2\pi}{3}} + i_c e^{j\frac{4\pi}{3}}\right)^*$$

$$= \left(\frac{2}{3}K\right)^2 \left[v_a i_a + v_b i_b + v_c i_c + j\frac{1}{\sqrt{3}}(v_a(i_c - i_b) + v_b(i_a - i_c) + v_c(i_b - i_a)\right] \tag{II.15}$$

From the real part, we get the active power expression.

$$P = \frac{3}{2K^2} Re\{v^s(i^s)^*\} = \frac{3}{2K^2} Re\{v^{dq}(i^{dq})^*\} = v_a i_a + v_b i_b + v_c i_c \tag{II.16}$$

From the imaginary part, we get the reactive power expression.

$$Q = \frac{3}{2K^2} Im\{v^s(i^s)^*\} = \frac{3}{2K^2} Im\{v^{dq}(i^{dq})^*\}$$

$$= \frac{1}{\sqrt{3}}[v_a(i_c - i_b) + v_b(i_a - i_c) + v_c(i_b - i_a)] \tag{II.17}$$

II.6. Principle of voltage-oriented control space vector modulation

The principle of control scheme is shown in Figure (II.6), which mainly consists of a PLL (Phase Locked Loop), PI decoupled controller, d- and q-axis component and PWM modulation [21].

VOC technique is based on the orientation of the current vector in the same direction as the voltage vector. When the line current vector $i = i_d + ji_q$ is aligned with the phase voltage vector $v = v_d + jv_q$ of the power line which supply the rectifier, the UPF condition is met. The switching signals a, b and c for each phase of the rectifier are generated by a space vector modulator SVM [22], then a dq-coordinate values with the DC-link voltage value are used in a decoupled controller.

Finally, the voltages created by the decoupled controller are sent to the PWM block to create switching patterns where S = 1 means upper switch ON and S=0 means lower switch ON.

According to the previous figure II.5, we will have three main parts in the model: the PLL block, a decoupled controller block composed of a current and voltage controller, a PWM block.

II.6.1. Phase locked loop

The PLL is a critical part in the system, it's a numeric method to calculate the electric angle θ of the three-phase system (U_a, U_b, U_c), which is necessary for the d-q transformation. This angle used by next in all coming dq-transformations in this model.

The PLL block designed according to [23]

$$\dot{\omega} = \gamma_1 \varepsilon \tag{II.18}$$

$$\dot{\theta} = \omega + \gamma_2 \varepsilon \tag{II.19}$$

γ_1 and γ_2 are gain parameters and ε is the error signal (γ_1 is the K_i, and γ_2 is the K_p of a PI controller), the error signal is selected E_q.

$$\gamma_1 = \frac{\rho^2}{\hat{E}_g}, \tag{II.20}$$

$$\gamma_2 = \frac{2\rho}{\hat{E}_g} \tag{II.21}$$

$$\hat{E}_g = \sqrt{\hat{E}_d{}^2 + \hat{E}_q{}^2} \tag{II.22}$$

Where ρ is the bandwidth of the PLL in rad/s and $\hat{E}_g$ is the grid voltage modulus. The PLL scheme is presented in figure II.6 [19].

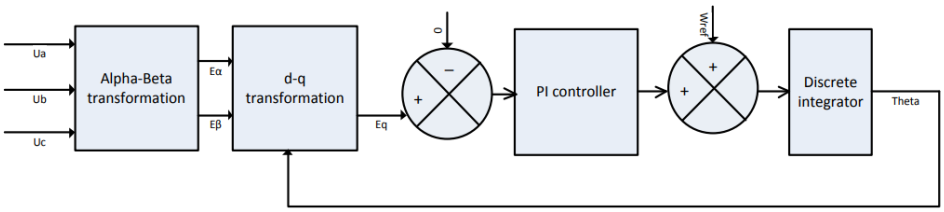

Figure II.7: PLL theoretical implementation scheme

II.6.2. Decoupled controller

The role of a decoupling controller is to separate or decouple the control of different variables in the system (current and voltage in our study), allows each variable to be independently and more effectively controlled. A schematic of decoupled controller is given in figure II.6 with the current controller and the dc-link voltage controller [9].

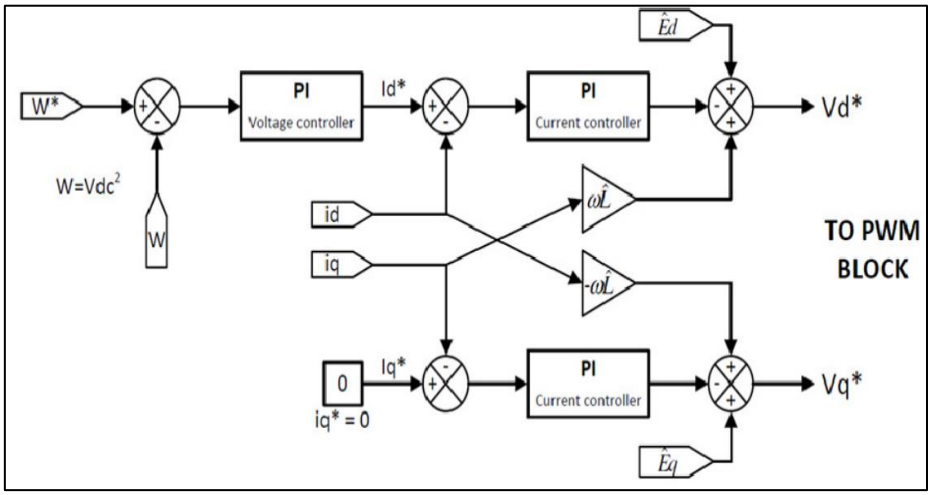

Figure II.8: current and dc-link voltage controller

II.6.2.1. Synchronous PI control

Synchronous PI control refers to Proportional-Integral controller in the synchronous (dq) reference frame, it's designed to removes error, provide fast dynamic response and high decoupling between the d and q axes.

From the schematic below, the synchronous coordinates equation (notation $x_{dq} = x_d + jx_q$) [19]:

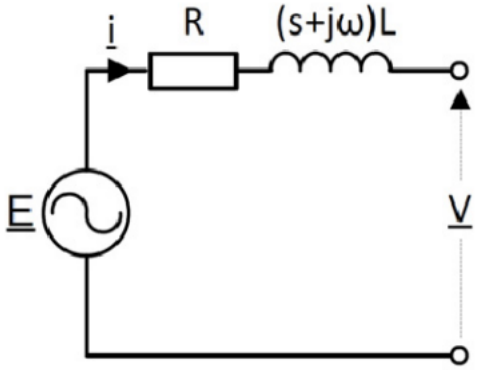

Figure II.9: synchronous PI control scheme [9]

$$L\frac{di_{dq}}{dt} = E_{dq} - (R + j\omega L)i_{dq} - v_{dq} \quad \text{(II.23)}$$

$$(R + sL + j\omega L)i_{dq} = E_{dq} - v_{dq} \quad \text{(II.24)}$$

$$\Rightarrow i_{dq} = \frac{E_{dq} - v_{dq}}{R + sL + j\omega L} \quad \text{(II.25)}$$

The system transfer function is

$$G_{dq}(s) = \frac{i_{dq}}{v_{dq}} = -\frac{1}{R + sL + j\omega L} \quad \text{(II.26)}$$

II.6.2.2. DC-link voltage controller

The DC-link voltage is modelled as a pure capacitor, where the electrical energy expression is [9].

$$E_c = \frac{1}{2}Cv_{dc}^2 \quad \text{(II.27)}$$

An error is sent to the controller by tracking the instantaneous voltage and comparing its square value with the reference voltage's square value [22].

$$\varepsilon = W_{ref} - W = V_{dc\,ref}^2 - V_{dc}^2 \quad \text{(II.28)}$$

The reference current i_d^* is calculated by applying PI control:

$$i_d^* = k_p\varepsilon + k_i\frac{\varepsilon}{s} \quad \text{(II.29)}$$

The PI control parameters (proportional and integral coefficients) are:

$$K_{pv} = \frac{\alpha_v C}{3E_m} \quad K_{iv} = 0.01$$

We will choose α_v at least a decade smaller than the current control bandwidth $\alpha_v < \frac{\alpha_i}{10}$

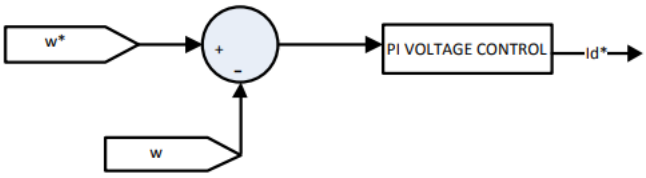

Figure II.10: DC –link voltage controller [19]

II.6.2.3. Current controller

Once a DC-link voltage is controlled, the reference current i_d^* is calculated. The implementation of the controller is done in two PI control loops, one for each component of the current i_d^* and i_q^*. The outputs of the two PI controls are respectively [19]:

$$V_d^* = E_d - k_p \varepsilon_d - k_i \frac{\varepsilon_d}{s} + \omega L I_q \qquad \text{(II.30)}$$

with $\varepsilon_d = I_d^* - I_d$

$$V_q^* = E_q - k_p \varepsilon_q - k_i \frac{\varepsilon_q}{s} + \omega L I_d \qquad \text{(II.31)}$$

with $\varepsilon_q = I_q^* - I_q$

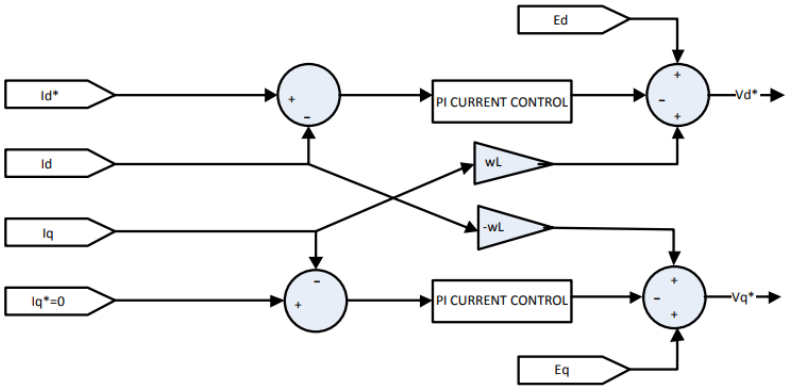

Figure II.11: Current controller block diagram

By cancelling the cross coupling initiated by the term $j\omega L i_{dq}$ in (II.24), the equation (II.25) becomes

$$i_{dq} = \frac{v_{dq}{}'}{R+sL} \tag{II.32}$$

$G_{dq}{}'(s)$ is the decoupled system transfer function written as follow:

$$G_{dq}{}'(s) = \frac{i_{dq}}{v_{dq}{}'} = \frac{1}{R+sL} \tag{II.33}$$

The first order transfer function of PI controller is:

$$F(s) = K_p + \frac{K_i}{s} \tag{II.34}$$

Based on IMC method of [23], we can write:

$$F(s) = \frac{\alpha_i}{s} G'^{-1}(s) = \frac{\alpha_i}{s}(R + sL) = \alpha_i L + \frac{\alpha_i R}{s} \tag{II.35}$$

The PI control parameters are $K_{pi} = \alpha_i L$ and $K_{ii} = \alpha_i R$, where α_i the current controller bandwidth is chosen a decade smaller than the switching frequency $\alpha_i = \frac{2\pi f_{sw}}{10}$ [9].

II.7. Sliding mode

The non-linear controller based on sliding mode is known to be robust against parametric uncertainties and external disturbance. The controller objective is to drive the plant state to the sliding surface and maintain it on the surface for all subsequent times [24]. PWM rectifier is a non-linear system, which creates the harmonics due to the distortion of the AC side current (harmonic pollution phenomenon) that increases the THD and reduces the input power factor. In this section we apply the sliding mode control in the voltage loop in order to linearize the studied system to reach the desired performances [17].

We consider a non-linear system as the following:

$$\dot{X}(t) = A(X,t) + B(X,t)U(t) \tag{II.36}$$

where, *A(X, t)* and ***B(X, t)*** are two non-linear functions, *X(t)* and *U(t)* are the state of the system and the control input respectively. The design of the sliding mode control is based on the choice of a sliding surface *S(X, t)*

II.7.1 Sliding surface design

For our rectifier model, we have the equation system (II.13):

$$\begin{cases} \dfrac{di_d}{dt} = -\dfrac{R}{L}i_d + \omega i_q + \dfrac{1}{L}(e_d - v_d) \\ \dfrac{di_q}{dt} = -\dfrac{R}{L}i_q + \omega i_d + \dfrac{1}{L}(e_q - v_q) \\ \dfrac{dv_{dc}}{dt} = \dfrac{-v_{dc}}{CR_L} + \dfrac{(e_d i_d + e_q i_q)}{Cv_{dc}} \end{cases}$$

Various forms of sliding surfaces are proposed in the literature, we define the sliding surface as [24]:

$$s(t) = \left(\lambda + \frac{d}{dt}\right)^{n-1} e(t) \tag{II.37}$$

where e(t) is a tracking error, and λ is strictly positive constant.

For n=1 $s(t) = e(t)$

For n=2 $s(t) = \lambda e(t) + \dot{e}(t)$

For output dc voltage tracking-problem, n is set to 1 and the sliding surface is designed as follows:

$$s(t) = e(t) = i_{d-ref} - i_d \tag{II.38}$$

$$\dot{s}(t) = i_{d-ref} - i_d = i_{d-ref} - (-\frac{R}{L}i_d + \omega i_q + \frac{1}{L}(e_d - v_d)) - \lambda sign(s) - \mu s \tag{II.39}$$

After simplification, we get

$$e_d = Li_{d-ref} + Ri_d - L\omega i_q + v_d + L\lambda sign(s) + L\mu s \tag{II.40}$$

Where μ is a positive constant, The function sign(s) denotes signum function defined as:

$$\text{Sign(s)} = \begin{cases} +1 \; if \; s > 0 \\ 0 \; if \; s = 0 \\ -1 \; if \; s < 0 \end{cases} \tag{II.41}$$

II.7.2 Stability analysis

This is to choose a candidate function of Lyapunov V(t) > 0 (positive function) for the state variables of the system and choose a command law that will decrease this function $\dot{v}(t) < 0$ Let us use the following Lyapunov function [24]:

$$V(t) = \frac{1}{2}s(t)^2 \tag{II.42}$$

The time derivative of V is given by:

$$\dot{V}(t) = s(t).\dot{s}(t) \tag{II.43}$$

For the Lyapunov candidate function to be able to decrease, it is enough to ensure that:

$$s(t).\dot{s}(t) < 0 \tag{II.44}$$

This approach is used to estimate the performance of the control, the study of the robustness and stability of nonlinear systems.

II.8. Conclusion

In conclusion, the voltage-oriented control is a complex algorithm that involves considering various components and factors. This chapter covers various control strategies, including direct and virtual flux power control (DPC and VF-DCP), voltage and virtual flux-oriented control (VOC and VF-VOC), the comparison of these control strategies reveals their efficiency in regulating output voltage, active and reactive power, and improving power quality. The choice of strategy depends on the system requirements, the VOC offers unique advantages in terms of high-power factor, near-sinusoidal current waveforms and harmonic reduction. Overall VO control guarantees both high dynamics and static performance via an internal current control loop, has become very popular and has constantly been developed and improved. To prove that, the coming chapter contain simulation of the controller and results to discuss.

Chapter III

Simulation and results

III.1 Introduction

To expose the performance of strategy voltage-oriented control VOC applied to a model of PWM rectifier, we present in this chapter the different results of numerical simulation, the PWM rectifier with the whole control scheme that designed in the previous section has been simulated using MATLAB-SIMULINK environment.

We will examine the performance of the following methods: voltage-oriented control VOC with PI controller rectifier and with sliding mode. For better assessment of each individual rectifier control technique presented, a comparative investigation of these techniques has been carried out.

III.2 First simulation result

To validate the effectiveness of the VOC control strategy studied in this work, a continuous simulation was carried out under MATLAB/SIMULINK environment with the following parameters presented in table III.1.

Table III.1 Parameters used in simulation study of VOC

Parameters	Value
L(H)	5e-3
R(Ω)	0.1
C(μF)	2200
Rload(Ω)	50
Kpi	62.8
Kii	12.60
Kpv	16.8
Kiv	64.152
Lω	1.57079
Vdc ref (V)	1000

The simulation with MATLAB Simulink gave the results shown in the following figures:

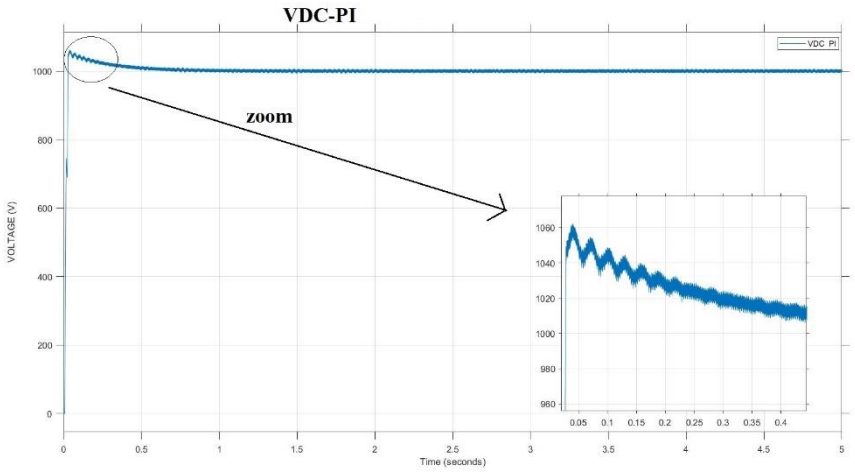

Figure III.1: Simulation result of the DC-link voltage

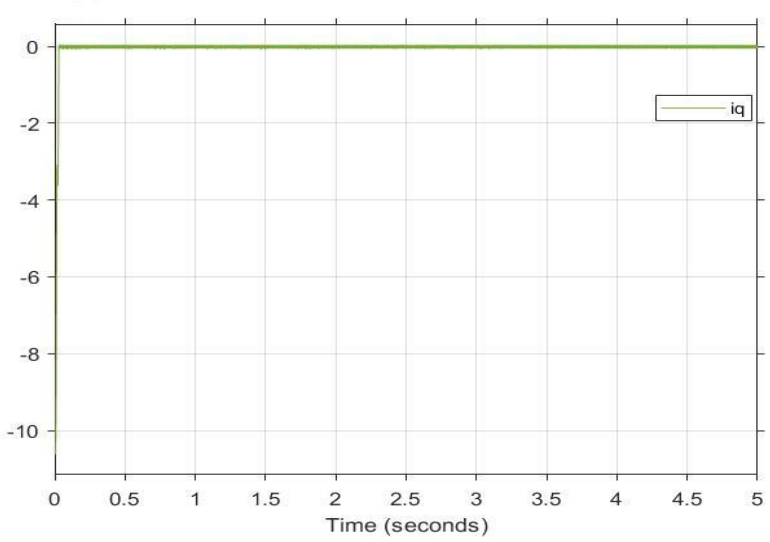

Figure III.2: Simulation results of the i_q current

III.2.1 Discussion and interpretation

Figure III.1 is the waveform of the DC link voltage, it shows that the output DC-link voltage after a short of response time approximately 0,9 s reaches the reference voltage 1000V. Figure III.1 is the zoomed of DC-link voltage which shows an error output less than 7V.

To operate the rectifier with unity power factor, the reference of i_q component is equal to null value as shown in figure III.2. The simulation results demonstrate that the voltage-oriented

control PWM rectifier can assure an accurate DC-link voltage and provide a sinusoidal AC current waveform.

III.3 Second simulation result

In this simulation a sliding mode technique is applied in voltage control of the decoupled controller instead of proportional integral control, the parameters of the system are the same as in table (III.1). The values of two constants λ and μ are given in the following table

Table III.2: Constant sliding mode values

Constant	Value
λ	2
μ	1000

The simulation with MATLAB Simulink gave the result shown in the following figures:

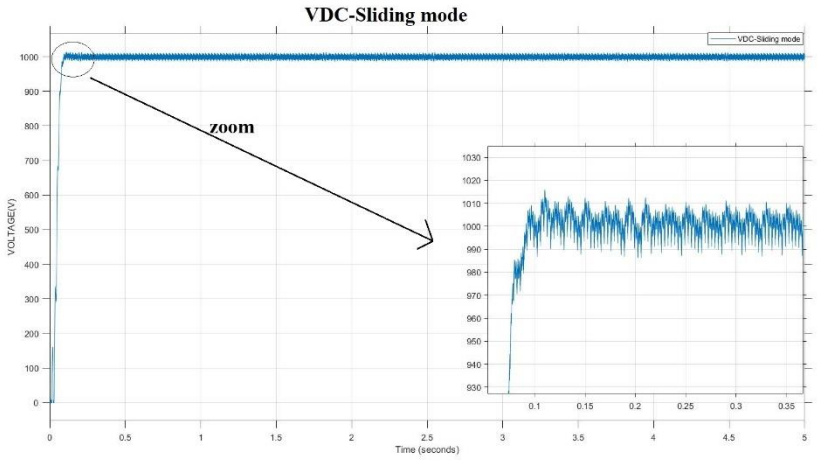

Figure III.3: Simulation result of the DC-link voltage with sliding mode

III.3.1 Discussion and interpretation

In this section, we show the feasibility and effectiveness of sliding mode with PI control. The figure III.3 represents the DC side voltage response, it shows that the output voltage has a good response and a very small response time around 0,1s to reaches the reference voltage 1000V and there is no overshoot in the response, according to the zoomed part the error output is around 10V.

III.4 Conclusion

For better assessment of each rectifier control technique presented, a comparative investigation of these techniques has been carried out. This issue is of great importance to designers and manufacturers. The two control schemes have been simulated using MATLAB/SIMULINK environment. The comparative study was conducted with respect to the complexity of control algorithms and their dynamic performance

The overall steady performances of the two control methods for PWM rectifier give a DC output voltage, however, for the VOC rectifier with sliding mode, the voltage quickly rises to around 1000V with no overshoot and minimal steady-state error. The DC-link voltage of VOC with the PI control technique has a lower error output in steady-state, longer time response and Larger initial overshoot. While the PI controller offers smoother and stable performance, the Sliding Mode Controller provides robustness, better disturbance rejection, and superior handling of nonlinearities. Thus, the VOC with SMC control technique seems to be the most advantageous.

General conclusion

There are plenty of applications for three-phase PWM rectifiers in power electronics, which is why researchers have long been interested in enhancing their control scheme. The aim of this work concerns the study, modelling and control of a system of three phase PWM rectifier based on voltage-oriented control to improve its performance such that the following criterion are utmost satisfied: sinusoidal and distortion-free line current, unity power factor, controllable and ripple free DC-link voltage. For this purpose, several control strategies for PWM rectifiers have been proposed and compared.

The initial chapter provides a comprehensive overview of three-phase controlled rectifiers, serves as an introductory foundation laying the groundwork for the subsequent in-depth exploration of three-phase PWM rectifiers, we deduced the input-and-output mathematical model of a three-phase PWM rectifier, established its simulation model in MATLAB/Simulink and then simulate the system. The results were satisfying, the adopted VOC technique showed excellent power achievement such as unity power factor by setting to zero the value of the reactive component of the current and synchronizing the currents in the system with the voltages, small error and better voltage regulation then other technique give in chapter three.

the PWM modulation method was implemented, although the modulation method could be improved using Space Vector Modulation. SVM is a simple and effective method gives a considerable reduction in harmonics, which meets modern grid power quality requirements

It can therefore, be concluded that the three-phase PWM rectifier, when combined with advanced voltage-oriented control strategies, offers a compelling solution for high-performance power conversion in a wide range of industrial applications.

References:

[1] Shrud, M. A. M. (2008). A systematic approach to the development of automotive electrical power system architectures (Doctoral dissertation, University of Derby).

[2] Wang, S. (2024, January 24). Active Front End (AFE). Technical notes. Updated on June 11, 2024

[3] Delta Electronics, Inc. (n.d.). Active Front End (AFE). Delta.from https://www.deltaww.com/en-us/products/06010501/ALL/

[4] Parvez, M., Mekhilef, S., Tan, N.M., & Akagi, H. (2015). An improved active-front-end rectifier using model predictive control. 2015 IEEE Applied Power Electronics Conference and Exposition (APEC), 122-127.

[5] Vani, E., & Rengarajan, N. (2016). Optimal operation of Low Cost Topology for Improving the Power Quality in the Wind Power Conversion System. Indonesian Journal of Electrical Engineering and Computer Science, 1(3), 523. https://doi.org/10.11591/ijeecs.v1.i3.pp523-533.

[6] Molligoda, D. A., Pou, J., Ceballos, S., Satpathi, K., Sasongko, F., Gajanayake, C. J., & Gupta, A. K. (2020). Current Distortion Mitigation in Grid-Connected Vienna Rectifier During Nonunity Power Factor Operation. IECON 2020 the 46th Annual Conference of the IEEE Industrial Electronics Society. https://doi.org/10.1109/iecon43393.2020.9255341.

[7] Liu, J., Wong, C. S., Li, Z., Jiang, X., & Loo, K. (2023). An Integrated Three-Phase AC–DC Wireless-Power-Transfer Converter With Active Power Factor Correction Using Three Transmitter Coils. IEEE Transactions on Power Electronics, 38, 7821-7835.

[8] MALINOWSKI MARIUSZ. “Sensorless Control Strategies for Three-Phase PWM Rectifiers”. PhD Thesis, Warsaw University of Technology, Faculty of Electrical Engineering, Institute of Control and Industrial Electronics. Warsaw, Poland. 2001. 128p

[9] Lechat, S. S. (2010). Voltage oriented control of three-phase boost PWM converters..

[10] NILSSON, Kristofer. Torque estimation of double fed induction generator using a dynamic model and measured data. CODEN: LUTEDX/TEIE-, 2010.

[11] Nilsson, K. (2010). Torque estimation of double fed induction generator using a dynamic model and measured data (Master's thesis).

[12] Kim, S. H. (2017). Electric motor control: DC, AC, and BLDC motors. Elsevier.

[13] Wang, C. (2017, February). Hysteresis Analysis of Three Phase Voltage Source PWM Rectifier based on Feed Forward Decoupling. In 2016 2nd International Conference on

Materials Engineering and Information Technology Applications (MEITA 2016) (pp. 20-26). Atlantis Press.

[14] Jamma, M., Barara, M., Akherraz, M., & Enache, B. A. (2016, June). Voltage oriented control of three-phase PWM rectifier using space vector modulation and input output feedback linearization theory. In 2016 8th International Conference on Electronics, Computers and Artificial Intelligence (ECAI) (pp. 1-8). IEEE.

[15] Malinowski, M. (2001). Sensorless control strategies for three-phase PWM rectifiers (Doctoral dissertation, Ph. D. Thesis Warsaw University of Technology Faculty of Electrical Engineering Institute of Control and Industrial Electronics. Warsaw, Poland).

[16] Fan, B., Wang, X. B., Yang, Z. X., Song, L., & Song, S. Z. (2017). Direct power control in pulse-width modulation rectifier based on virtual flux estimation. Advances in Mechanical Engineering, 9(5), 1687814017699142.

[17] BARKAT, Said, TLEMÇANI, Abdelhalim, et NOURI, Hassan. Direct power control of the PWM rectifier using sliding mode control. International Journal of Power and Energy Conversion, 2011, vol. 2, no 4, p. 289-306.

[18] MALINOWSKI, Mariusz, KAZMIERKOWSKI, Marian P., HANSEN, Steffan, et al. Virtual-flux-based direct power control of three-phase PWM rectifiers. IEEE Transactions on industry applications, 2001, vol. 37, no 4, p. 1019-1027.

[19] CARMONA, Daniel Castro et MANDIOLA, Javier Fernández. Design and implementation of a Three-Phase Boost Battery Charger with PFC using CompactRIO control system. 2012.

[20] Prasad, S. S., & Vikram, C. (n.d.). Space vector modulation based three-phase PWM rectifier voltage oriented control. Journal of Emerging Technologies and Innovative Research

[21] YIN, Hang et DIECKERHOFF, Sibylle. Experimental comparison of DPC and VOC control of a three-level NPC grid connected converter. In : 2015 IEEE 6th International Symposium on Power Electronics for Distributed Generation Systems (PEDG). IEEE, 2015. p. 1-7.

[22] MALINOWSKI, Mariusz, KAZMIERKOWSKI, Marian P., et TRZYNADLOWSKI, Andrzej M. A comparative study of control techniques for PWM rectifiers in AC adjustable speed drives. IEEE Transactions on power electronics, 2003, vol. 18, no 6, p. 1390-1396.

[23] OTTERSTEN ROLF. “On Control of Back-to-Back converters and Sensorless Induction Machine Drives”. PhD Thesis, Department of Electric Power Engineering, Chalmers University of Technology, Göteborg, Sweden. 2003. 165p. ISBN: 91-7291-296-0.

[24] ROUABHI, Riyadh. Contrôle des puissances générées par un système éolien à vitesse variable basé sur une machine asynchrone double alimentée. 2016. Thèse de doctorat. Université de Batna 2.